Melting of Snow Cover in a Tropical Mountain Environment in Bolivia: Processes and Modeling

Yves Lejeune, Ludovic Bouilloud, Pierre Etchevers, Patrick Wagnon, Pierre Chevallier, Jean-Emmanuel Sicart, Eric Martin, Florence Habets

Melting of Snow Cover in a Tropical Mountain Environment in Bolivia: Processes and Modeling

YVES LEJEUNE,* PATRICK WAGNON,+ LUDOVIC BOUILLOUD,* PIERRE CHEVALLIER,#
PIERRE ETCHEVERS,* ERIC MARTIN,@ JEAN-EMMANUEL SICART,# AND FLORENCE HABETS&

*Centre d'Etude de la Neige, Météo-France/CNRM, Saint Martin d'Hères, France
+Great Ice, Laboratoire de Glaciologie et de Géophysique de l'Environnement, Institut de Recherche pour le Développement, Saint Martin d'Hères, France
#Great Ice, Maison des Sciences de l'Eau, Institut de Recherche pour le Développement, Montpellier, France
@Météo-France/CNRM/GMME, Toulouse, France
&UMR-SISYPHE ENSMP, Fontainebleau, France

(Manuscript received 13 July 2006, in final form 16 October 2006)

ABSTRACT

To determine the physical processes involved in the melting and disappearance of transient snow cover in nonglacierized tropical areas, the CROCUS snow model, interactions between Soil–Biosphere–Atmosphere (ISBA) land surface model, and coupled ISBA/CROCUS model have been applied to a full set of meteorological data recorded at 4795 m MSL on a moraine area in Bolivia (16°17′S, 68°32′W) between 14 May 2002 and 15 July 2003. The models have been adapted to tropical conditions, in particular the high level of incident solar radiation throughout the year. As long as a suitable function is included to represent the mosaic partitioning of the surface between snow cover and bare ground and local fresh snow grain type (as graupel) is adapted, the ISBA and ISBA/CROCUS models can accurately simulate snow behavior over nonglacierized natural surfaces in the Tropics. Incident solar radiation is responsible for efficient melting of the snow surface (favored by fresh snow albedo values usually not exceeding 0.8) and also for the energy stored in snow-free areas (albedo = 0.18) and transferred horizontally to adjacent snow patches. These horizontal energy transfers (by conduction within the upper soil layers and by turbulent advection) explain most of the snowmelt and prevent the snow cover from lasting more than a few days during the wet season in this high-altitude tropical environment.

1. Introduction

In the South American Andes, a large fraction of the population living west of the mountain range relies on glacier melt and snowmelt for water supply, irrigation, and hydropower. At certain high Andean sites, clear evidence of global warming trends over recent decades has been found in oxygen isotope values extracted from ice cores (Thompson et al. 2003). Moreover, global circulation models predict a 2.5°C temperature increase over the next ~80 yr for this tropical mountain zone (Bradley et al. 2004). This strong warming will have a major effect on glacier- and snow-supplied river water resources, and consequently the population and economies of the region will have to make tremendous adjustments (Barnett et al. 2005; Chevallier et al. 2004). The shrinkage of tropical glaciers has been well documented and increasingly observed since the end of the 1970s in the central Andes (e.g., Wagnon et al. 2001; Kaser and Osmaston 2002; Francou et al. 2003; Favier et al. 2004; Sicart et al. 2005). However, although the impact of snow cover on the water supply is nonnegligible, the evolution and variability of snow cover on nonglacierized areas have not, to our knowledge, been studied on a local scale in this region.

This present study focuses on the melting of the snow cover on a moraine site located at 4795 m MSL in the Charquini area (Bolivia, 16°17′S, 68°32′W) of the tropical Andes. Snowmelt is calculated by applying the energy balance to a control volume of snow, using a detailed and comprehensive set of meteorological data (Lejeune et al. 2003, 2006). The energy balance of the snowpack and the evolution of the snow cover are

Corresponding author address: Yves Lejeune, Centre d'Etude de la Neige, Météo-France, 1441 rue de la Piscine, 38400 Saint Martin d'Hères, France.
E-mail: yves.lejeune@meteo.fr

DOI: 10.1175/JHM590.1

simulated three ways: 1) using the CROCUS model (Brun et al. 1989, 1992; Durand et al. 1999) and, since the ground flux at this site is strong and highly variable, 2) using the ground Interactions between Soil–Biosphere–Atmosphere (ISBA) (Noilhan and Planton 1989), and 3) coupled ISBA/CROCUS models. The objectives of this study are to apply these models to the particular climatic conditions encountered in the Tropics, in order to assess their performance and provide insight into the physics and energy budget of a high-altitude tropical snowpack.

The paper is divided into five parts. Section 2 deals with the experimental setting, including the energy balance and climatic conditions of this high-altitude site. Section 3 describes the models and the main adjustments that were made in applying them to this tropical site. Section 4 presents various simulations corresponding to different events with snow on the ground, with a step-by-step discussion of further model adjustments made and their results. A subsection devoted to model comparison is also included. The paper ends with a discussion and conclusions (section 5).

2. Experimental setting, energy balance, and climatic conditions

a. Location

The experimental site is located in Bolivia, in the Cordillera Real, about 30 km north of the capital La Paz, at 4795 m MSL (16°17′S, 68°32′W). Figure 1 shows a map of the region with the location and a photograph of the automatic weather station (AWS) used in this study. The Cordillera Real is a natural barrier between the wet and low Amazon basin and the dry and high Altiplano. The AWS is located on the northeast flank of Cerro Charquini (5392 m MSL), on a natural flat area of an average 15° slope facing the Zongo valley and the high Amazon basin, and around 100 m lower in altitude than the snout of Charquini Glacier. The Charquini area is located about 5 km immediately southeast of Huayna Potosi where the Zongo Glacier has been studied over the last 15 yr (Fig. 1) (e.g., Wagnon et al. 2001; Sicart et al. 2005). The AWS stands on ranker-type soil, the top 0.50 m containing roughly 70% sand, 20% loam, and 10% clay. The soil is never frozen. The superficial layer (0.02 m) contains a significant proportion of organic matter (32%). The surface is made of debris of various sizes (rocks from about 0.10 to 1 m in diameter) mixed with short, sparse vegetation (mainly sparse high-altitude grass), covering less than 30% of the surface.

b. Experimental setting

Table 1 lists the sensors of the AWS. The meteorological variables are recorded as half-hourly means with a 10-s time step, except for wind direction (instantaneous values every 30 min) and precipitation (cumulative sum every 10 min).

The precipitation phase (liquid or solid) is evaluated using air temperature thresholds: if $T_{\text{air}} \leq -1°\text{C}$, precipitation is snow; if $T_{\text{air}} \geq +3°\text{C}$, precipitation is rain; and if $-1°\text{C} < T_{\text{air}} < +3°\text{C}$, an algorithm based on a number of variables (albedo, ground heat flux, surface and air temperatures) and their variations between the beginning and the end of each time step has been developed and checked against field observations to distinguish between snow and rain (Lejeune et al. 2006; L'Hôte et al. 2005). Complementary observations (cloud cover, cloud types, snow depth, density and water content, crystal type, etc.) were carried out during various field trips made throughout the studied period (45 days in all). Every morning between May 2002 and July 2003, an observer took pictures of the site to obtain the fraction of the ground covered by snow.

Since the ultrasonic sensor did not work properly for intervals during the entire period the snow depth was not always available (only 427 hourly measurements seem to be acceptable, taken into account during the 10 247 h of the entire period). Surface albedo measurements are therefore used to identify the events with snow on the ground. For this reason, a dimensionless parameter, referred to as diffalb (diffalb = hourly measured albedo − hourly bare soil albedo; where mean hourly bare soil albedo value = 0.18), has been used during the daytime. This parameter, varying from 0 to values close to 0.8, can be used to check whether there was snow on the ground (when diffalb > 0) or not (when diffalb $= 0$), crucial for model validation. The maximum values as high as 0.8 occur only during snowfalls, when the incident solar radiation sensor is covered by snow (in such cases, relating to 2.5% of the diurnal hours, measured hourly albedo is limited to 1).

c. Energy balance

With such an experimental dataset (based on an hourly time step over the entire measurement period extending from 14 May 2002 to 15 July 2003, and made up of precipitation, air temperature, humidity, wind velocity, and incoming shortwave and longwave radiations), the models are able to accurately determine the energy budget (EB) of the snowpack or the atmosphere–ground interface (when the soil is snow free) according to

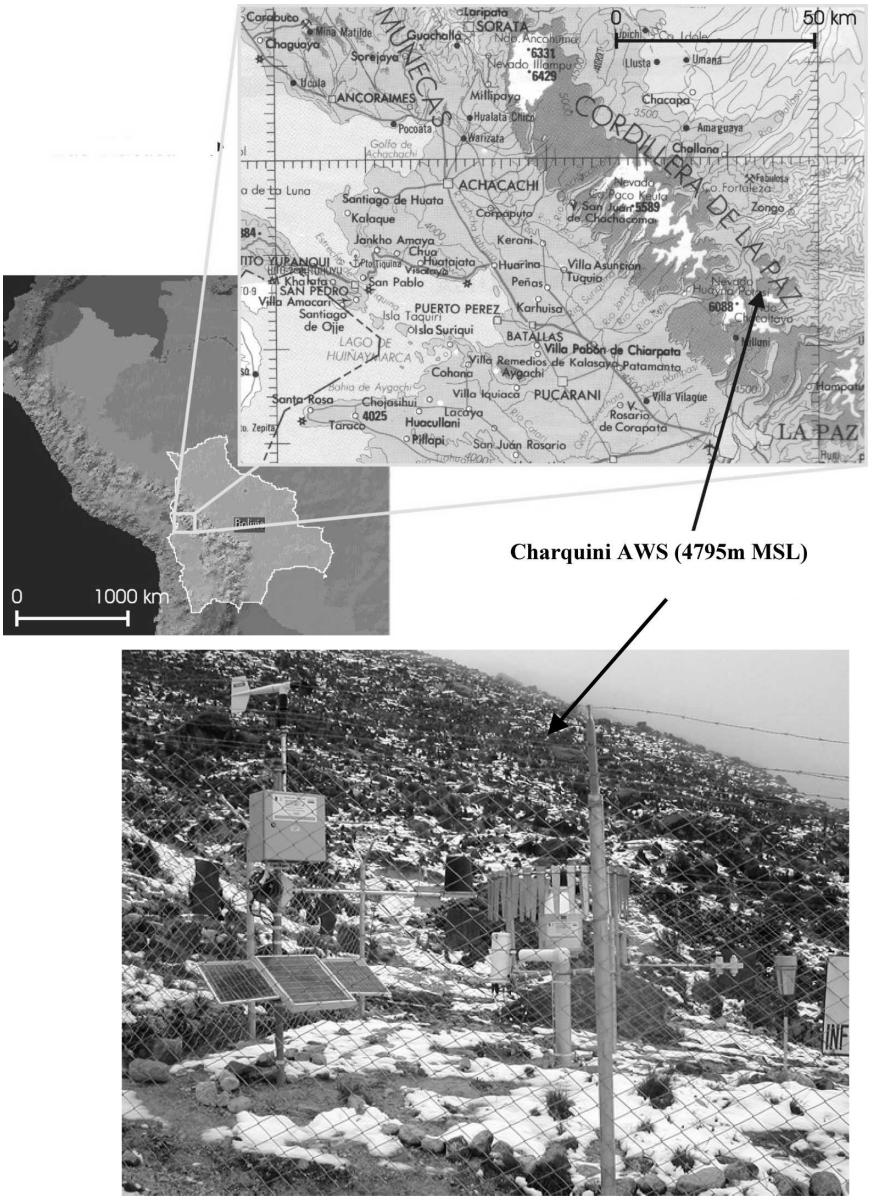

FIG. 1. Location map of the measurement site, showing the Charquini area and the Zongo Glacier, and a picture of the AWS site with patchy snow cover.

$$\mathrm{EB} = \mathrm{SW_{in}}(1 - \alpha) + \mathrm{LW_{in}} + \mathrm{LW_{out}} + \mathrm{LE} + H + G + Q_p (\mathrm{W\ m^{-2}}), \quad (1)$$

where $\mathrm{SW_{in}}$ is the incident solar radiation; α is the snow (or bare ground) surface albedo; $\mathrm{LW_{in}}$ and $\mathrm{LW_{out}}$ are the incoming and outgoing longwave radiation fluxes, respectively; LE and H are the turbulent latent and sensible heat fluxes, respectively; G is the ground heat flux; and Q_p is the energy flux supplied by precipitation. Note that fluxes directed toward the snowpack or the snow-free ground surface are positive by convention. If the soil is snow free, EB = 0, and if not, EB corresponds to the snowpack energy variation per unit time. Note that G presented here is not only the geothermal flux, but also includes the conductive heat flux within the superficial layers of the soil due to the energy stored in the ground (produced by atmospheric and geothermal fluxes).

d. Climatic conditions

The mean values of the recorded meteorological variables over the entire measurement period (14 May 2002–15 July 2003) are displayed in Table 1. Figure 2

TABLE 1. List of AWS sensors installed at 4795 m MSL and mean values (or total precipitation) of the various meteorological variables over the entire measurement period (14 May 2002–15 Jul 2003).

Quantity	Sensor type (height)	Accuracy	Mean value (14 May 2002–15 Jul 2003)
Precipitation (kg m^{-2})	Géonor T-200B (1.75 m) Elsyde R013030A (1.2 m) Totalizer (1.4 m)	$\pm 0.1\ 10^{-3}$ kg m^{-2} $\pm 0.2\ 10^{-3}$ kg m^{-2}	Snow total: 924 kg m^{-2} Rain total: 378 kg m^{-2}*
Air temperature (°C)	Vaisala HPM45C–aspirated (1.5 m)	±0.2°C	1.65°C
Relative humidity (%)	Vaisala HPM45C–aspirated (1.5 m)	±2% on (0%–90%) ±3% on (90%–100%)	68.7%
Wind speed (m s^{-1})	Young 05103 (2.05 m)	±0.3 m s^{-1}	Modulus: 1.3 m s^{-1}
Wind direction (deg)	Young 05103 (2.05 m)	±3 deg	
Incident and reflected shortwave radiation (W m^{-2})	Kipp & Zonen CM3 (0.9 m) $0.305 < \lambda < 2.8 \times 10^{-6}$ m	±10% on the daily sum	Incident: 198 W m^{-2} Reflected: 42.3 W m^{-2}
Incoming and outgoing longwave radiation (W m^{-2})	Kipp & Zonen CG3 (0.9 m) $5 < \lambda < 50 \times 10^{-6}$ m	±10% on the daily sum	Incoming: 276 W m^{-2} Outgoing: —**
Ground temperature (°C)	Cu-Cst thermocouples (−0.03, −0.10, −0.20 and −0.43 m)	±0.2°C	−0.03 m: 5.2°C −0.10 m: 5.0°C −0.20 m: 5.1°C −0.43 m: 5.0°C
Ground flux (W m^{-2})	Hukseflux HFP01 (−0.03 m)	60μV/(W m^{-2})$^{-1}$	−1.7 W m^{-2}
Accumulation/ablation* (m)	Campbell UDG01 ultrasonic depth gauge (1.15 m)	$\pm 10^{-2}$ m	—**

* No value for the Totalizer is provided due to irregular measurements during the field campaign.
** There are many gaps in the dataset for outgoing longwave radiation and accumulation/ablation.

shows their daily averages over the period. More details concerning the meteorological and snow database can be found in Lejeune et al. (2003, 2006).

The Charquini area is located in the outer Tropics (Kaser 2001), characterized by homogeneous temperature conditions and an annual wet and dry season. Figures 2a and 2b show that daily air temperature varies only slightly throughout the year, whereas the relative humidity and precipitation show strong seasonal variations. The winter dry season (May–August) is produced by the northward displacement of the mid- and upper-tropospheric westerlies, which in turn prevent moisture influx from the east. On the other hand, the wet season (October–March), during which the most significant snowfalls occur over the high Andean mountains, is a result of the seasonal expansion of the equatorial easterlies in the upper troposphere, allowing near-surface moisture influx from the east (Garreaud 2000; Vuille et al. 2000).

One special feature of high tropical mountains is the very intense incident solar radiation SW_{in} (Fig. 2c) during the wet season (austral summer) compared to SW_{in} in the Alps during the boreal winter (Lejeune et al. 2006), preventing the snow cover from lasting more than a few days on moraine areas. In contrast to Alpine thick seasonal snow cover lasting a number of months, the snow cover over nonglacierized areas of the tropical Andes is more transient and the wet season is marked by few-hour to few-day snow episodes on the ground alternating with periods of bare ground. During these periods without snow on the ground, a large part of the incident solar radiation is absorbed by the low-albedo surface (~0.18). Figure 2d also displays the daily ground heat flux (G_{-3}) measured 0.03 m below the surface. Hourly G_{-3} values (not shown) are almost constant and equal to 10 W m^{-2} when the surface is covered by snow (e.g., 30 June–6 July 2002, 28–30 July 2002, and 16–17 October 2002), and are highly variable the rest of the time, especially when there is snow on the ground only a few hours a day (50 days out of the 183 days of the wet season), and when snow accumulation and melting are synchronous as it is usual in the Tropics. Then, G_{-3} oscillates from positive hourly values at night, reaching 50 W m^{-2}, to negative diurnal hourly values as low as −200 W m^{-2}. The Charquini site is very calm with a mean wind velocity of 1.3 m s^{-1} over the entire measurement period and a daily mean maximum not exceeding 4.4 m s^{-1} (Fig. 2d).

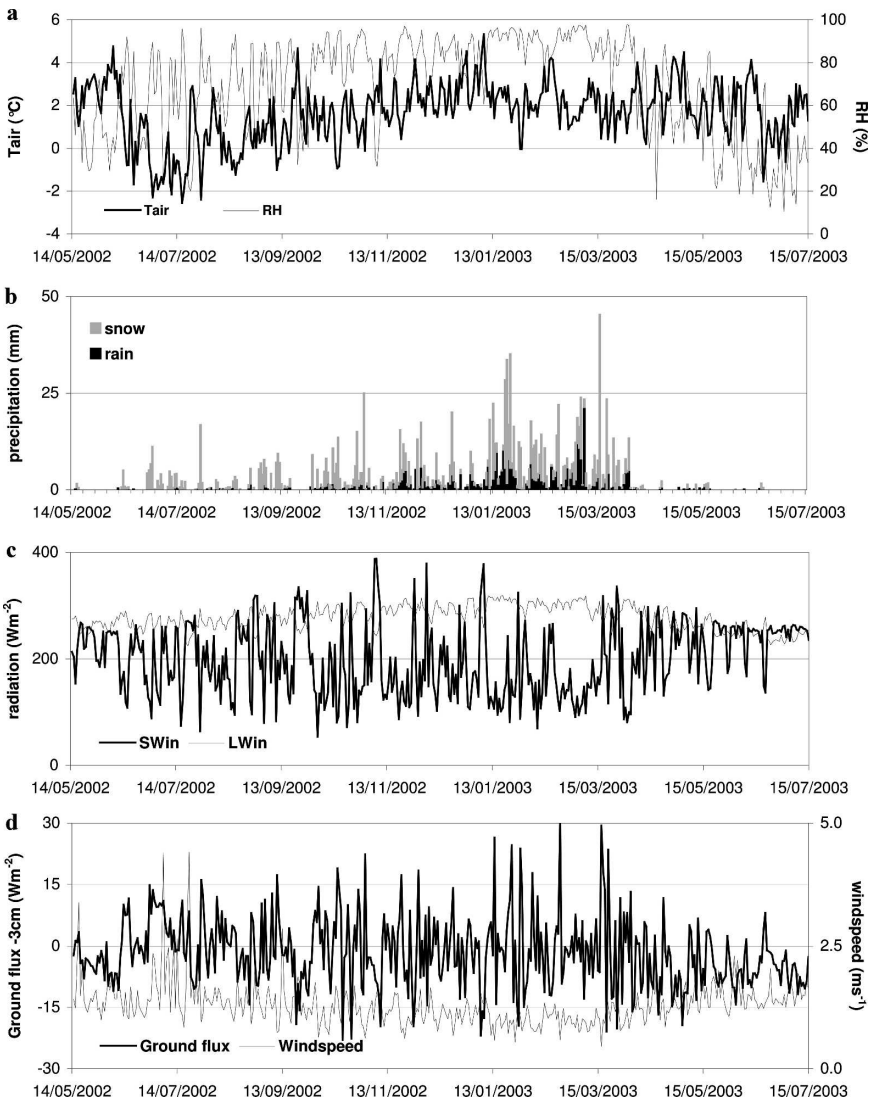

FIG. 2. Variation in the daily mean values of (a) air temperature (T_{air}), relative humidity (RH), (b) daily cumulative solid (gray histograms) and liquid precipitation (black histograms), (c) incident solar radiation (SW_{in}), incoming longwave radiation (LW_{in}), and (d) ground heat flux at 0.03 m below the ground surface and wind velocity over the measurement period (14 May 2002–15 Jul 2003).

3. Model description

a. The CROCUS model

CROCUS is a one-dimensional multilayer physical model of the snow cover developed for operational avalanche forecasting (Brun et al. 1989, 1992). It explicitly evaluates mass and energy exchanges between the snowpack and the low-level atmosphere at 15-min time steps as a function of meteorological conditions, including turbulent heat and moisture surface transfers, and ground heat flux (which remains low in the European Alps). The number of layers simulated by the model varies from 1 to 50. It computes the heat transfer within the snowpack and also the grain types (the snow surface albedo is calculated as a function of snow surface grain types, based on optical diameter), snow temperature, density, and liquid-water content for each snow layer. Although the CROCUS model was initially developed to simulate seasonal snow in the Alps (e.g., Durand et al. 1999; Etchevers et al. 2003), it has been successfully applied to glaciers in the Alps (Gerbaux et al. 2005) and at high latitudes (Dang et al. 1997). It has however never been tested in a tropical environment.

b. The ISBA model

The one-dimensional model ISBA describes at 5-min time steps the exchanges of heat and water between the low-level atmosphere, soil, snow, and vegetation (Noilhan and Planton 1989, Noilhan and Mahfouf 1996). As ISBA is designed for global circulation models it is a relatively simple scheme; however, it embraces the most important components of the land surface processes. Since its initial development, various applications have led to new versions. In this paper, we use 1) the diffusion version for soil and soil freezing parameterization (Boone et al. 2000; Bazile 1999), which allowed calculation of the full vertical profile of soil temperature, liquid water, and ice content, and 2) the snow cover parameterization, which is the multilayer snow scheme developed and compared to CROCUS at the Col de Porte site in the French Alps (1320 m MSL, 45°30′N, 5°77′E) by Boone and Etchevers (2001). Although not as accurate as CROCUS in the simulation of the internal state of snowpack, it appears to provide a good compromise between accuracy and computational cost for an application not focused on snow alone. This version of ISBA has been used for the Project for the Intercomparison of Land-Surface Parameterization Schemes Phase 2(e) [PILPS2(e)] test on a Scandinavian basin (Habets et al. 2003), for the Snow Models Intercomparison Project (SnowMIP; Etchevers et al. 2003) and for the whole upper valley of the Zongo River, where the Charquini AWS is located, in order to improve water resource management for hydropower generation (Caballero et al. 2004).

c. The coupled ISBA/CROCUS model

To precisely describe the snow cover and thermal and water exchanges at the snow–soil interface, the coupled ISBA/CROCUS model is used in this paper. This coupled model was originally developed for the forecasting of snow occurrence on roads, and subsequently adapted to our case. This coupling method, described in detail in Bouilloud and Martin (2006), makes it possible to use the detailed CROCUS model for the snow and the more advanced parameterization of ISBA for the soil description. It also includes some specific parameters for capillary rise in the snow under certain conditions and for the thermal resistance at the interface, depending on the snow and upper soil temperature, ice, and liquid content. Developed for winter road maintenance, the ground surface considered by ISBA/CROCUS is not covered by vegetation and as soon as there is snow on the roads, the model considers that snow uniformly covers the ground. The coupled model was checked against observations during a comprehensive experimental campaign over three winters at the Col de Porte site (Bouilloud and Martin 2006). During this campaign, the coupled model proved that it was able to accurately simulate the rapid heat flux variations between the snow and the experimental road.

d. Soil parameters used in ISBA and coupled ISBA/CROCUS models for the present study

Soil properties are derived from sand and clay proportions using the standard ISBA parameterization. These proportions were roughly estimated in the upper 50 cm during the field campaign and applied to the whole soil layer (70% sand and 10% clay). The corresponding values of the dry soil density, volumetric porosity, and water-saturated thermal conductivity are 1540 kg m^{-3}, 42% (considered to be water saturated), and 1.9 W m^{-1} K^{-1}, respectively. The dry heat capacity is taken to be equal to 733 J kg^{-1} K^{-1} (Peters-Lidard et al. 1998). The bare soil albedo used in the simulations is 0.18, in agreement with the mean value measured by the AWS, and ground emissivity is assumed to be 0.95 (Noilhan and Planton 1989). The soil surface roughness length is assumed to be 0.025 m, as proposed by Liston and Sturm (1998). Results do not have a very big influence on this last parameter since wind speed was always very low and the surface energy balance was mainly governed by radiative fluxes. Since the vegetation cover is very sparse at this site, the main ISBA and ISBA/CROCUS runs were carried out without any vegetation cover. Nevertheless, an ultimate ISBA test assuming a proportion of soil covered by 30% vegetation will be briefly presented in order to check if the sparse vegetation cover on the site could have any impact on the results. The impact of the fraction of the ground covered by snow (F_S) will be discussed in the following section.

4. Model simulations and statistical evaluation

To simulate the evolution of the snow cover, we proceed step by step: 1) starting with the CROCUS snow model as used for conditions prevailing in the Alps, and then adding adjustments related to the special features of tropical climate, 2) continuing with the coupled ISBA/CROCUS model including (or not) a horizontal snow–ground partitioning factor F_S, and 3) ending with the ISBA model. The main characteristics of each run are summarized in Table 2. All the following simulations, presented for an hourly time step, were per-

TABLE 2. Main characteristics of each run presented in the text.

Run number	Model	Fresh snow albedo parameterization*	Snow–ground partitioning**	% of bare ground covered by vegetation
Run 1	CROCUS	No	No	0
Run 2	CROCUS	Yes	No	0
Run 3	CROCUS/ISBA	Yes	F_{S_new}	0
Run 3 bis	CROCUS/ISBA	Yes	No	0
Run 4	ISBA	Yes	F_{S_new}	0
Run 4 bis	ISBA	Yes	F_{S_sta}	0
Run 4 veg	ISBA	Yes	F_{S_new}	30

* This parameterization refers to section 4b.
** This parameterization refers to sections 4c, 4d, and 4e.

formed over the entire measurement period, but for the sake of clarity, only parts of the entire period are displayed on the figures. These selected periods illustrate the important snow cover events of the whole measurement period for which the greatest number of snow depth measurements are available and for which the determination of precipitation phases is the most dependable.

a. Run 1: CROCUS model as used in the Alps

Only one adjustment was made to the initial CROCUS model: instead of using the ground flux model developed for winter in the Alps, with values from 0.5 to 2.5 W m^{-2} depending on site elevation (Brun et al. 1989), the ground flux was increased to a constant value of 10 W m^{-2}. This takes into account the high ground flux (section 2d and Fig. 2) measured on the site compared to the average daily ground heat fluxes encountered in Northern Hemisphere regions that generally fall in the range from 0 to 4.6 W m^{-2} (Pomeroy et al. 1998). Figures 3b,d show the snow depths simulated by run 1 for more than one month during the 2002 dry season (27 June–1 August 2002) and one-and-a-half months during the 2003 wet season (16 February–4 April 2003), as well as available measured snow depths. Daily precipitation and the hourly diffalb parameter are plotted in Figs. 3a,c. Note that the model largely overestimates the snow depth for two reasons: first, some of the snow depth increases are overestimated and second, the simulated depletion is too slow—leading to a quasi-permanent snow cover over both seasons, which is totally different from the real situation (illustrated by the large number of diffalb values equal to 0). The overestimation does not come from errors in density estimations. Indeed, the simulated fresh snow densities (from 130 to 175 kg m^{-3} depending on snowfalls) are slightly lower than densities measured in the field (sometimes as high as 230 kg m^{-3}); however, snow density measurements were performed over impermeable snowboards and thus tend to overestimate the true density because of the artificially increased water content of the snow. In some cases, the precipitation phase was not properly evaluated, as for example on 17 March 2003 where part of the rain was interpreted as snow, leading to an excessively thick simulated initial snow cover. Fortunately such cases are rare, as demonstrated in the validation of the phase determination method by Lejeune et al. (2006). A detailed analysis of each snow cover event shows that the model only simulates snow depth increases during snowfall, without any concomitant melting. In reality, as said before, accumulation and melting are synchronous, explaining why the true snow depth is lower than the values simulated by run 1. The overestimation of snow depth at the beginning of snow events causes the simulation to deviate from measurements, a problem that is reinforced by the fact that simulated melting after snowfalls is too slow [e.g., the simulated depletion of the snowpack after the snowfalls of 30 June 2002 and 29–30 July 2002 (Fig. 3b) is much slower than in reality].

b. Run 2: CROCUS model with initial grain-type parameters adapted to the Tropics

In the Alps, winter snowfalls are mainly due to cold fronts producing small dendritic crystals, whereas snowfalls in Bolivia are usually of convective origin, resulting in bigger round crystals of graupel type. The CROCUS model (Brun et al. 1992) uses the following parameter settings to describe this type of crystal: dendricity = 0, sphericity = 1, and diameter = 1 mm (as measured in the field), which means that fresh crystals are considered to be perfect 1-mm-diameter spheres in the model. This change in CROCUS settings implies values of fresh-snow albedo almost never exceeding 0.8 compared to values in the Alps often higher than 0.9. This low albedo value is consistent with observations

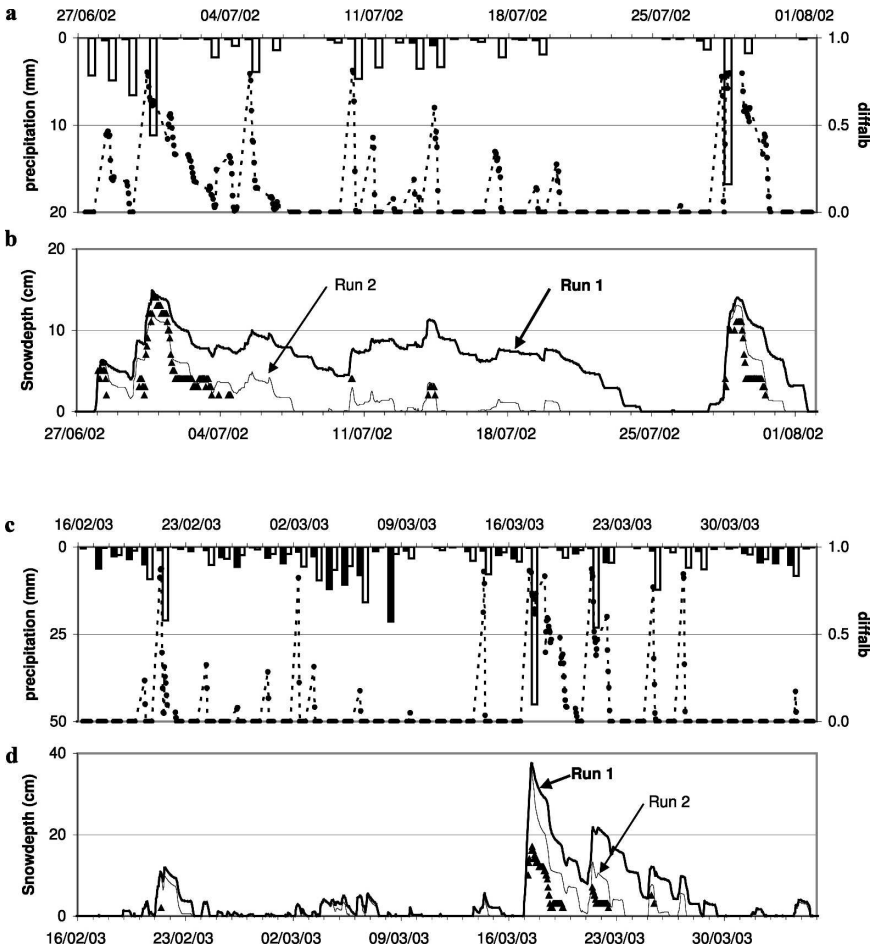

FIG. 3. Simulated snow depth from run 1 (solid thick line) and run 2 (solid thin line) compared to measured snow depth (solid triangles) for two periods: (b) 27 Jun–1 Aug 2002 during the dry season and (d) 16 Feb–4 Apr 2003 during the wet season. (a), (c) Also shown are the daily cumulative values of solid (white histograms) and liquid precipitation (black histograms), and the dimensionless parameter diffalb (dotted line with black points) (diffalb = daily mean albedo − measured bare soil albedo). Run 1 and run 2 are discussed in text sections 4a and 4b, respectively.

and with previous work carried out on Zongo Glacier (e.g., Wagnon et al. 2001). Moreover, the albedo of snow with rounded grains decreases more quickly than for dendritic snow (diffalb fall is obviously significant in Figs. 3a,c). Figures 3b,d display a comparison between run 1 and run 2 over the studied dry- and wet-season periods. The new settings better reproduce depletion once the snow cover has been established. This means that the albedo of the snow cover of the Bolivian Andes is lower than in the Alps (due to the different type of fresh crystals) and is responsible for faster melting due to enhanced absorption of incident solar radiation. This crucial role of albedo for melting on tropical glaciers has already been pointed out (e.g., Wagnon et al. 2001; Favier et al. 2004). In spite of this improvement, the number of hours with snow on the ground in the daytime is still overestimated in run 2 (1285 h) compared to reality (587 h).

c. *Run 3: Snow cover simulations with coupled ISBA/CROCUS model*

To determine if better simulation of the duration of the snow cover requires better estimation of the energy input from the ground, we performed a test using the CROCUS model with settings similar to those of run 2 and a ground heat flux forced to the value measured at 0.03 m below the ground surface. In this test, the duration of the snow cover and the depletion of the snowpack are far better reproduced over the entire measurement period, indicating that accurate simulation of the ground heat transfers is a crucial issue in this study. Consequently, the CROCUS snow model was coupled

with the ISBA ground model to correctly take into account not only heat exchanges with the snow but also energy transfers to the ground.

1) SNOW–GROUND PARTITIONING F_S

On natural surfaces with thin snow cover, the surface usually appears as a mosaic of patches of snow and bare ground due to surface irregularities such as rocks of various sizes or vegetation clusters. To compute this natural snow patching, a fraction of the ground surface covered by snow (F_S) is included in the ISBA model. Roesch et al. (2001) or Essery and Pomeroy (2004) suggest various formulations for the F_S fraction depending on size-scale applications. The standard ISBA function F_{S_sta} (appropriate for large-scale applications, such as the GCM use) is based on the water equivalent of the snowpack and is expressed as (Etchevers 2000; Boone and Etchevers 2001)

$$F_{S\_sta} = \frac{SWE}{SWE + SWE_{crit}}, \quad (2)$$

where SWE (kg m^{-2}) is the snow water equivalent over patches covered by snow and SWE_{crit} is a calibrated parameter (equal to 10 kg m^{-2}). In our case, where vegetation is sparse and snow water equivalent measurements too irregular, a sharper function (more suitable for local-scale applications), fraction F_{S_new}, is used in the coupled ISBA/CROCUS model. This new fraction depends only on snow depth, which is easier to measure than water equivalent. It is expressed as

$$F_{S\_new} = MIN\left[1, \left(\frac{H}{H_{crit}}\right)\right]^x, \quad (3)$$

where H is the simulated snow height (in meters), and H_{crit} and x are model parameters; H_{crit} is a critical snow height (in meters) above which the ground is totally covered by snow (state never reached with the standard ISBA function). According to the function suggested by Brun et al. (1994), the power x was added to better represent reality, where the fraction of the snow cover is not a linear function of snow height. To calibrate the F_{S_new} parameters H_{crit} and x, a sensitivity test was performed to obtain a best fit for observations of snow height when available as well as the presence of snow or not on the ground on an hourly time scale during the daytime. In this test, the parameters were varied within a reasonable physical range: 0.05, 0.075, and 0.1 m for H_{crit} and ⅓, ½, 1, 2, and 3 for x. The best set of parameters was also chosen to be in good agreement with field observations: H_{crit} = 0.1 m and x = ⅓. To show

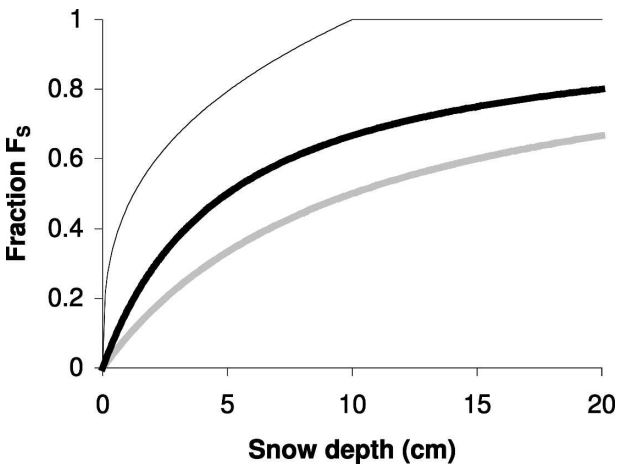

FIG. 4. Fraction of the ground surface covered by snow (F_S) as a function of snow depth (cm). The standard ISBA fraction F_{S_sta} is plotted for two snow densities: 200 kg m^{-3} (thick black line) and 100 kg m^{-3} (thick gray line), while the thin black line refers to the new fraction F_{S_new}.

the difference between the two expressions, F_{S_sta} (for two snow densities: 200 and 100 kg m^{-3}) and F_{S_new} (which is independent of snow density), are plotted as a function of snow depth in Fig. 4. When the snow layer is 2 cm (5 cm) thick, 60% (79%) of the ground is covered by snow with F_{S_new} compared to only 29% (50%) with F_{S_sta} (for a snow density equal to 200 kg m^{-3}) or 17% (33%) (for a snow density equal to 100 kg m^{-3}). The difference between the two expressions is relatively high, especially for small snow densities, but the F_{S_new} expression agrees better with field measurements and daily pictures. Although the sensitivity test performed to obtain the F_{S_new} fraction is not described in detail here, the relative impact of the two functions will be examined in the following section.

2) SNOW DEPTH SIMULATIONS

In run 3, the snow cover is computed by the coupled ISBA/CROCUS model including the F_{S_new} snow–ground partitioning function and the grain-type parameter settings selected for CROCUS run 2 (Table 2). Figure 5 presents examples of simulations over two periods: 30 August to 14 September 2002 and 12 October to 4 November 2002. The plotted hourly snow depth is the snow depth computed over snow-covered patches weighted by F_{S_new}. In Figs. 5b,e, for both periods, we see that the run-3 snow depth noticeably differs from run-2 simulations. On 11 September 2002 (Fig. 5b) and 31 October 2002 (Fig. 5e), run 3 better reproduces the snow depth increase than run 2. Furthermore, the depletion and duration of the snowpack are better simulated in run 3 than in run 2, suggesting that snow-

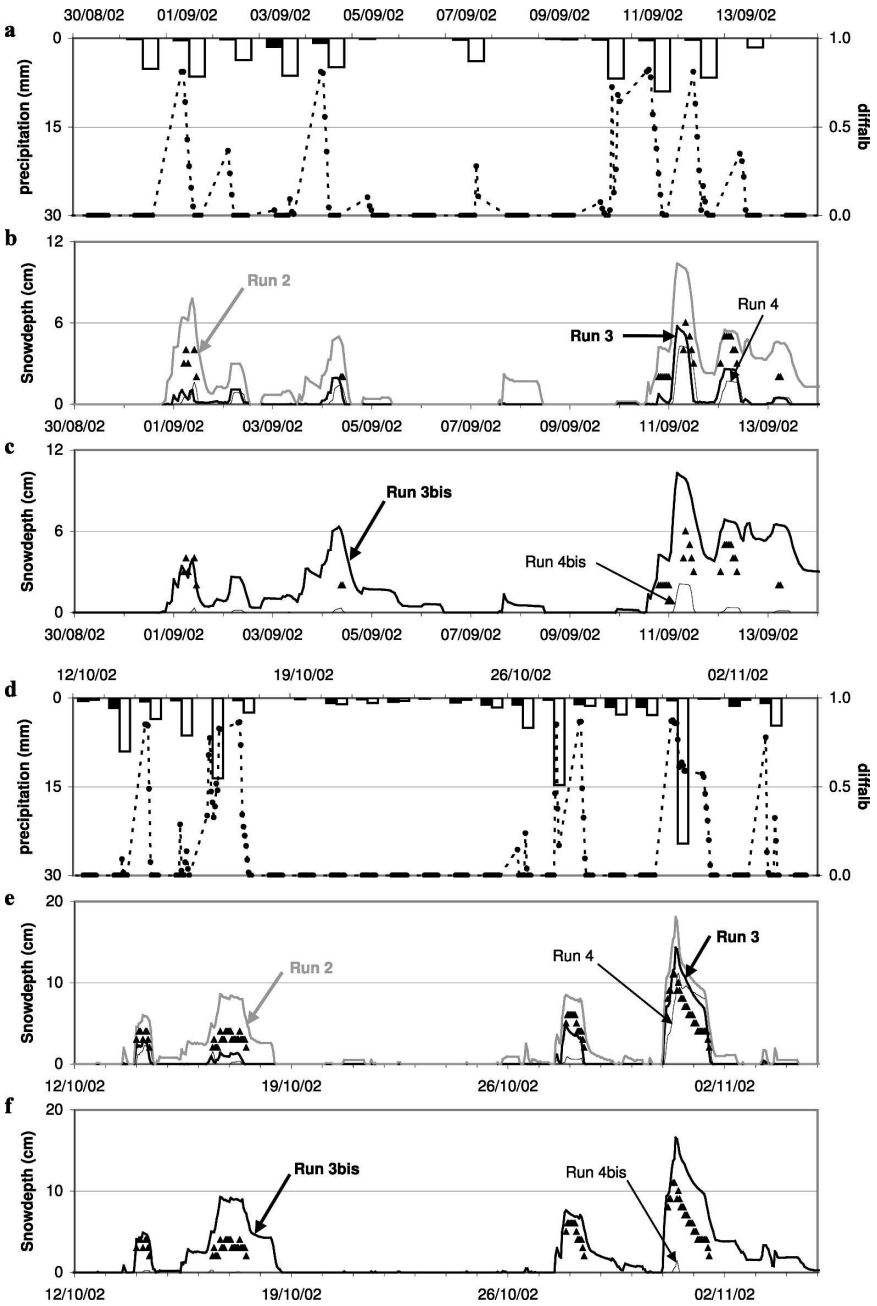

FIG. 5. A comparison of snow depth simulations with run 2 (thick gray line), run 3 (thick black line), and run 4 (thin black line) over the periods (b) 30 Aug–14 Sep 2002 and (e) 12 Oct–4 Nov 2002. (c), (f) Also displayed over the same periods are snow depth simulations with run 3bis (thick line) and run 4bis (thin line). (b), (c), (e), (f) Also shown are the measured snow depth (black triangles), the daily cumulative solid (white histograms), and liquid precipitation (black histograms), and (a), (d) the diffalb parameter (dotted line with black points).

melt is likely to be accelerated when the model takes into account heat transfers into the ground and a suitable snow–ground partitioning.

An additional CROCUS/ISBA run (run 3bis) was performed without any snow–ground partitioning. The poor and unrealistic snow depth simulations (Figs. 5c,f), marked by overestimated snow accumulation and excessive snow cover duration, show the importance of taking into account a patchy snow cover. In conclusion, the coupled ISBA/CROCUS model is able to accu-

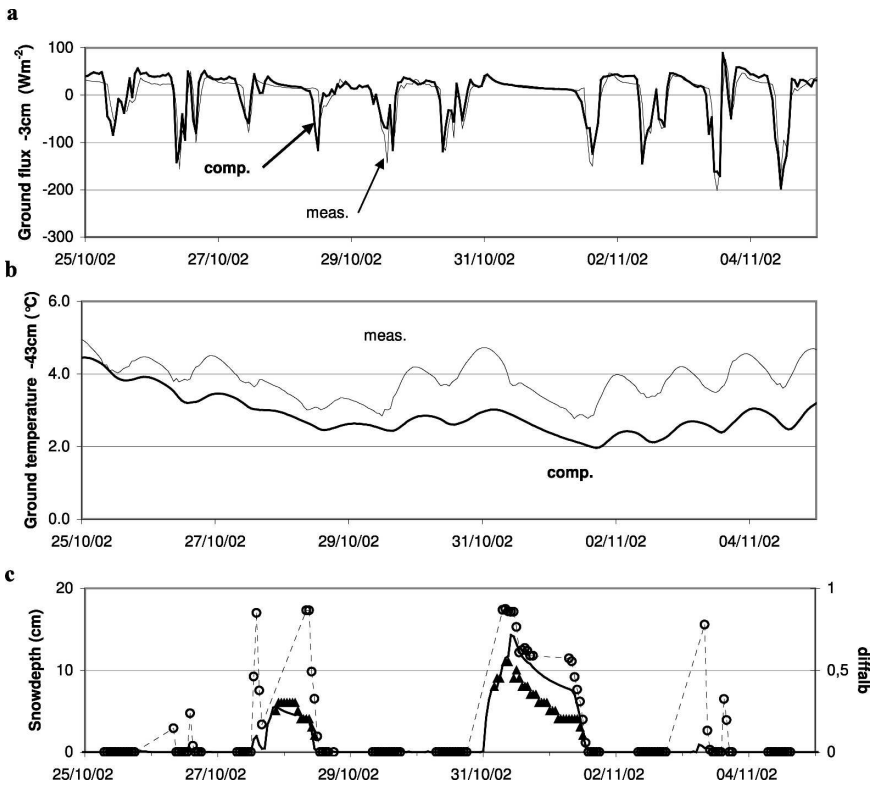

FIG. 6. (a) Comparison between the ground heat flux measured at 0.03 m below the surface on an hourly time scale (thin line) and the values computed by ISBA/CROCUS (run 3) in the layer located between 0.025 and 0.0375 m below the surface (thick line) over the period 25 Oct–4 Nov 2002. (b) Comparison of the measured (thin line) and computed (thick line) hourly soil temperatures at 0.43 m below the ground surface over the same period. (c) Measured (filled triangles) and simulated (solid line) snow depths with run 4 as well as the diffalb parameter over the same period (dashed line with circles).

rately simulate the snow cover under tropical conditions as long as a suitable snow–ground partitioning function is included.

3) VALIDATION: COMPARISON BETWEEN RUN-3-SIMULATED AND OBSERVED GROUND HEAT FLUX, GROUND TEMPERATURE, AND ALBEDO

It would have been of interest to systematically compare the snow depth measured by the ultrasonic sensor to the value simulated by CROCUS/ISBA run 3; however, this was not possible due to sensor breakdowns. Therefore, observed and run-3-simulated ground heat flux and temperature have been compared. Figure 6 displays the ground heat flux measured at 0.03 m below the surface on an hourly time scale and the values computed (ISBA/CROCUS run 3) in the layer located between 0.0250 and 0.0375 m below the surface over the period 25 October to 4 November 2002. Also shown are the measured and computed hourly soil temperatures at 0.43 m below the ground surface. Over this period (265 h), as shown in Table 3, the mean measured and simulated ground heat fluxes at −0.03 m are 1.0 and 4.0 W m^{-2} respectively (root-mean-square error of 26.1 W m^{-2}), and the mean measured and simulated ground temperatures at −0.43 m are 3.8° and 2.9°C respectively (root-mean-square error of 1.1°C). Moreover, measured and simulated mean albedos for the same period (99 h with measurements for which the sensor was not covered by snow) are 0.26 and 0.30, respectively (root-mean-square error of 0.12). Table 3 also displays comparisons between computed and measured ground heat fluxes at −0.03 m, ground temperature at −0.43 m, and surface albedo for three other well-documented snow events. The good agreement between heat fluxes, soil temperatures, and albedo shows that the coupled ISBA/CROCUS model is able to correctly reproduce not only the snow behavior over natural high-altitude tropical surfaces but also the physical processes involved in the snowpack and in the superficial soil.

TABLE 3. Comparison between measured (meas.) and ISBA/CROCUS-run 3 computed (comp.) ground heat fluxes at −0.03 m, ground temperatures at −0.43 m, and surface ground (snow + bare soil) albedo for four snow events. Mean values (mean) over the snow events and root-mean-square errors (rmse) are displayed.

			Ground heat flux at −0.03 m (W m^{-2})		Ground temperature at −0.43 m (°C)		Albedo*	
Snow events	No. of hours		meas.	comp.	meas.	comp.	meas.	comp.
Event 1 27 Jun–16 Jul 2002	457	Mean	5.9	5.7	2.5	2.4	0.37	0.28
		Rmse	44.3		0.4		0.14	
Event 2 26 Jul–2 Aug 2002	169	Mean	2.0	3.9	3.3	3.2	0.37	0.29
		Rmse	51.0		0.4		0.15	
Event 3 25 Oct–5 Nov 2002	265	Mean	1.0	4.0	3.8	2.9	0.26	0.30
		Rmse	26.1		1.1		0.12	
Event 4 13 Mar–5 Apr 2003	553	Mean	1.0	2.1	4.8	3.1	0.26	0.41
		Rmse	33.7		1.9		0.26	

* The number of hours for which albedo was measured (albedo < 1) was 173, 61, 99, and 212 h for snow events 1–4, respectively.

d. *Run-4 ISBA including F_{S_new} and F_{S_sta} snow–ground fractions*

The performance characteristics of the coupled CROCUS/ISBA model (run 3) and the ISBA model (run 4) were also compared. The standard version of ISBA was used, including the snow cover scheme (simpler than CROCUS) developed by Boone and Etchevers (2001) and using the F_{S_new} fraction instead of the standard F_{S_sta} fraction (Table 2). Vegetation cover was neglected here. Moreover, as for the initial grain-type settings adopted for run 3, the fresh snow albedo was fixed to 0.8. As seen in Figs. 5b,e, it appears that snow depth simulations of run 3 and run 4 agree well for the most significant snow events. This means that ISBA including the calibrated F_{S_new} fraction is also a suitable tool to reproduce Charquini snow cover.

To test the sensitivity of the ISBA model to the choice of the F_S fraction, a run 4bis simulation corresponding to the ISBA model including the standard snow–ground fraction F_{S_sta} is also presented in Figs. 5c,f. The thickness and the duration of the resulting simulated snow cover are by far underestimated, due an unrealistic proportion of snow patches (underestimated) and snow-free patches (overestimated). This test clearly shows that the ISBA model is very sensitive to the choice of the snow–ground partitioning parameters, which thus plays a key role in the duration of the snow cover.

e. *A comparative analysis of the performance of each run using the Rousseau index*

The Rousseau index examines the ability of a model to correctly reproduce reality (Rousseau 1980). This statistical index is commonly used in meteorology to compare predicted and observed datasets (e.g., Durand et al. 1998). The Rousseau index I is expressed as

$$I = \frac{\mathrm{SO} \times \mathrm{NSNO} - \left(\frac{\mathrm{NSO} + \mathrm{SNO}}{2}\right)^2}{\left(\mathrm{SO} + \frac{\mathrm{NSO} + \mathrm{SNO}}{2}\right) \times \left(\mathrm{NSNO} + \frac{\mathrm{NSO} + \mathrm{SNO}}{2}\right)}, \quad (4)$$

where SO is the number of "snow presence on ground" events simulated and observed, SNO is the number of events simulated but not observed, NSO is the number of events not simulated but observed, and NSNO is the number of events neither simulated nor observed. This index varies between −1 (nil simulating) and 1 (perfect simulating). Unlike classical indexes (ratio test, threat score . . .), its nonlinear formulation makes it more constraining and systematically penalizes biased computations.

Here, to study the performance of each run (summarized in Table 2), we compare the measured and simulated occurrences of snow on the ground during the day. In the daytime, there is effectively snow on the ground when diffalb > 0 and no snow on the ground when diffalb = 0. For the simulations, there is snow on the ground when the calculated snow depth is strictly higher than 0 m. This comparison has been done only for daytime periods with snowfalls (10 snow events of 7 to 31 days, i.e., 1685 h in all), which means that long

TABLE 4. Comparison of the respective performance of each run for the occurrence of snow or not on the ground, on an hourly time scale during the daytime [run number and main characteristics (model, partitioning . . .) are summarized in Table 2]. The mean Rousseau indexes are also indicated for each model. Each Rousseau index in Table 4 is a mean Rousseau index for the 10 snow events weighted by the number of hours for each event. Snow events are the following: 27 Jun–16 Jul 2002 (184 h); 26 Jul–2 Aug 2002 (71 h); 16 Aug–16 Sep 2002 (330 h); 29 Sep–20 Oct 2002 (221 h); 25 Oct–5 Nov 2002 (121 h); 19 Nov–7 Dec 2002 (193 h); 19–25 Dec 2002 (68 h); 9–19 Jan 2003 (114 h); 3–16 Feb 2003 (147 h); and 13 Mar–5 Apr 2003 (236 h).

			Measurements (h)		
			Snow	No snow	Rousseau index
Simulations (h)	Run 1	Snow	452	651	0.17
		No snow	2	580	
	Run 2	Snow	449	344	0.53
		No snow	5	887	
	Run 3	Snow	367	153	0.64
		No snow	87	1078	
	Run 3 bis	Snow	443	597	0.21
		No snow	11	634	
	Run 4	Snow	320	97	0.62
		No snow	134	1134	
	Run 4 bis	Snow	249	84	0.51
		No snow	205	1147	
	Run 4 veg	Snow	315	94	0.62
		No snow	139	1137	

periods without snowfalls and with bare ground have been removed. Such periods (mainly for the dry season) would have artificially improved the performance of the models. Inversely, the event of 22–31 January 2003 has also been removed because the initial snow depth on 22 January was incorrect due to an obviously erroneous determination of the precipitation phase. Given that our goal in this section is to analyze the ability of each model to properly simulate snow behavior over natural surfaces and not to examine the ability of the algorithm to distinguish rain and snow, this case was not taken into account. Table 4 gives the results of this comparison for each run as well as the respective Rousseau indexes. Actually, the Rousseau index in Table 4 is a mean Rousseau index of the 10 snow events weighted by the number of hours for each event.

Similar Rousseau indexes higher than 0.6 (0.64 for CROCUS/ISBA run 3 and 0.62 for ISBA run 4) confirm that coupled CROCUS/ISBA and ISBA models using the F_{S_new} fraction are able to accurately simulate snow behavior during the day. Looking at the good agreement between observed and run-3-simulated ground heat fluxes and temperatures, and the good agreement between run 3 and run 4, we can reasonably assume that models also simulate snow behavior well at night. Moreover, the number of hours with erroneous simulations [simulated snow cover, although the ground is bare in reality (case SNO) and inversely (case NSO)] is much more balanced for ISBA/CROCUS run 3 and ISBA run 4 than for CROCUS run 2: 153 or 97 h (SNO case) and 87 or 134 h (NSO case) for run 3 or run 4, respectively, compared to 344 h (SNO case) and 5 h (NSO case) for run 2. This means that CROCUS run 2 tends to systematically underestimate melting, which explains why the snow cover lasts longer than in reality, which is not the case for run 3 and run 4.

In addition, a final run (run 4-veg) was performed with ISBA including F_{S_new} snow–ground partitioning and a proportion of soil covered by 30% of vegetation with a leaf area index of 0.5. The corresponding Rousseau index of 0.62 (Table 4), equal to run-4 Rousseau index, shows that the vegetation can easily be neglected for the Charquini site.

Finally, low Rousseau indexes for run 3bis and run 4bis (0.21 and 0.51, respectively) confirm the conclusion stated in sections 4c and 4d concerning the necessity of including a snow–ground partitioning function in these models.

5. Discussion and conclusions

Before moving on to further discussions, the snow sublimation contribution to snow cover evolution should first be specified, as this is an important mass- and energy-loss process on tropical glacier surfaces (snow or ice) (e.g., Wagnon et al. 2001; Mölg and Hardy 2004). In fact, during the entire experimental period, sublimation mass loss is close to 1% of the snowmelt (~0.1% and ~5% in wet and dry seasons, respectively), and sublimation energy loss is close to 6% of the positive energy budget allowing the snowmelt (~1% and ~15% in wet and dry seasons, respectively). Such conclusions show that over the Charquini moraine areas, where wind speed is quite low and air humidity during the wet season (the preferential period of snow cover constitution) is high, sublimation effects on snow cover evolution are of minor importance compared with net solar radiation or ground flux contributions.

This study shows that the coupled ISBA/CROCUS and ISBA models, including a suitable snow–ground partitioning function and adapted to natural soils and Bolivian conditions, are powerful tools to simulate snow behavior over nonglacierized natural surfaces in the Tropics. The comparisons between run 3, run 3bis, run 4, and run 4bis show that models are very sensitive to the snow–ground partitioning parameterization. These physical models have been successfully checked

against independent measurements such as ground heat flux at 0.03 m below the ground surface or 0.43-m-deep soil temperature. Although these models are one-dimensional, the addition of a horizontal snow–ground partitioning function virtually adds a second dimension, making it possible to take into account horizontal surface heterogeneities of mass and energy fluxes. Consequently, the special features of these models can provide insight into the energy budget of a high-altitude tropical snowpack and the physical processes involved in its melting.

Some of the important adjustments for the models are the initial settings for fresh snow crystals, here considered to be 1-mm-diameter spheres. This graupel-type fresh snow is consistent with the convective precipitation observed in Bolivia. The main effects of these settings are to reduce the fresh snow albedo from values higher than 0.9 in colder environments such as the Alps in winter to a maximum value of approximately 0.8 here, and to accelerate snow grain metamorphism. In this high-altitude tropical climate, where incident solar radiation is almost twice as high in winter or at the beginning of spring as in the Alps, albedo is a crucial parameter responsible for more efficient absorption of solar radiation and thus enhanced melting.

In addition, melting of the snowpack occurs not only at the surface but also at its bottom due to a strong ground heat flux, as supported by the accurate ISBA/CROCUS (run 3) and ISBA (run 4) simulations. It is therefore fundamental to take horizontal heterogeneities into account in mass and energy fluxes. Indeed, in high-altitude tropical nonglacierized areas, when there are snow events, the ground remains partly covered by wet snow most of the time. In such cases, at daytime, low-albedo surfaces of bare patches favor the absorption of the intense solar radiation, the temperature of the upper ground layers free of snow increases considerably, and so does the temperature of the air in the vicinity of the surface. Meanwhile, over snow patches, snow and near-interface ground temperatures are close to the melting point (0°C), implying a large horizontal temperature gradient not only in the top layers of the soil but also in the air immediately above the snow-covered and bare patches. Consequently, we can assume that horizontal energy transfers (not computed by the one-dimensional models used in this study), conduction in the soil, and advection in the air (partly accounted for as the measured air temperature will be influenced by warming over bare ground) are probably very strong during the daytime, and therefore responsible for the main part of snowmelt (through the ground heat flux at the base and the sensible heat flux on the surface of the peripheral snow cover). This process is inhibited as soon as snowfalls are sufficiently intense to deposit a layer thick enough (around 0.10 m) to totally cover the ground. Investigations such as those by Takahara and Higuchi (1985) and Granger et al. (2006) provide insight into the thermal modification of the air over melting patchy snow, and Essery et al. (2006) present a simple model for advection of heat over snow and soil patches.

In conclusion, in high-altitude nonglacierized tropical areas, intense incident solar radiation is responsible for both efficient melting at the snow surface (favored by moderate values of fresh snow albedo) and an important energy intake on bare surfaces (albedo = 0.18), transferred horizontally by conduction in the soil or by heat advection in the air. Although these processes are not directly simulated by models, they are very efficient and prevent lasting snow cover in these regions. Indeed, the snow cover over nonglacierized areas of the tropical Andes is transient and the wet season is marked by few-hour to few-day snow-on-the-ground events alternating with periods of snow-free ground. To better document the horizontal energy transfers between snow and bare ground, and to quantify the energy fluxes, detailed meteorological experiments conducted simultaneously over snow and bare patches are necessary (e.g., Granger et al. 2006).

Over the high Andean mountains, a seasonal snow cover can exist only on glaciers where the snow bottom flux and horizontal energy transfers (except on the edges) are low. To better understand the difference in snow cover evolution over bare ground (moraine) and glacier, further research work could measure, simulate, and compare the snowpack of both of these environments.

Acknowledgments. This work was sponsored by the French Project PNRH 01-37 involving IRD, Météo-France, and South American partners (UMSA, IHH, COBEE) who are gratefully acknowledged. A large part of this study is based on extensive field work carried out by J. P. Chazarin, E. Berthier, B. Francou, R. Gallaire, P. Garreta, R. Fuertes, A. Rabatel, and A. Soruco. The authors address special thanks to Y. L'Hôte, recently retired, for his consistent efforts in constituting a database. We also thank J. Noilhan, A. Coudrain, and P. Ribstein for useful discussions related to this article.

REFERENCES

Barnett, T. P., J. C. Adam, and D. P. Lettenmaier, 2005: Potential impacts of a warming climate on water availability in snow-dominated regions. *Nature,* **438,** 303–309.

Bazile, E., 1999: Soil water freezing in ISBA. *HIRLAM Newsletter,* No. 33, 92–95.

Boone, A., and P. Etchevers, 2001: An intercomparison of three snow schemes of varying complexity coupled to the same land surface and macroscale hydrologic models. *J. Hydrometeor.,* **2,** 374–394.

——, V. Masson, T. Meyers, and J. Noilhan, 2000: The influence of the inclusion of soil freezing on simulations by a soil–atmosphere–transfer scheme. *J. Appl. Meteor.,* **39,** 1544–1569.

Bouilloud, L., and E. Martin, 2006: A coupled model to simulate snow behavior on roads. *J. Appl. Meteor. Climatol.,* **45,** 500–516.

Bradley, R. S., F. T. Keimig, and H. F. Diaz, 2004: Projected temperature changes along the American Cordillera and the planned GCOS Network. *Geophys. Res. Lett.,* **31,** L16210, doi:10.1029/2004GL020229.

Brun, E., E. Martin, V. Simon, C. Gendre, and C. Coleou, 1989: An energy and mass model of snow cover suitable for operational avalanche forecasting. *J. Glaciol.,* **35,** 333–342.

——, P. David, M. Sudul, and G. Brunot, 1992: A numerical model to simulate snow-cover stratigraphy for operational avalanche forecasting. *J. Glaciol.,* **38,** 13–22.

——, V. Spiridonov, and E. Martin, 1994: Intégration d'un modèle de neige muti-couches dans ARPEGE: Interêts, approche méthodologique et premiers résultats. *Proc. Atelier de Modélisation de l'Atmosphère du CNRM, Météo-France,* Toulouse, France, Météo-France/CNRM, 133–140.

Caballero, Y., P. Chevallier, R. Gallaire, and R. Pillco, 2004: Flow modelling in a high mountain valley equipped with hydropower plants: Rio Zongo Valley–Cordillera Real–Bolivia. *Hydrol. Processes,* **18,** 939–957.

Chevallier, P., B. Pouyaud, and W. Suarez, 2004: Climate change impact on the water resources from the mountains in Peru. *Proc. OECD Global Forum on Sustainable Development: Development and Climate Change,* Paris, France, OECD, 11 pp. [Available online at http://www.oecd.org/dataoecd/37/20/34692989.pdf.]

Dang, H., C. Genthon, and E. Martin, 1997: Numerical modeling of snow cover over polar ice sheets. *Ann. Glaciol.,* **25,** 170–176.

Durand, Y., G. Giraud, and L. Mérindol, 1998: Short-term numerical avalanche forecast used operationally at Météo-France over the Alps and Pyrenees. *Ann. Glaciol.,* **26,** 357–366.

——, ——, E. Brun, L. Mérindol, and E. Martin, 1999: A computer-based system simulating snowpack structures as a tool for regional avalanche forecasting. *J. Glaciol.,* **45,** 469–484.

Essery, R., and J. Pomeroy, 2004: Implications of spatial distributions of snow mass and melt rate for snow-cover depletion: Theoretical considerations. *Ann. Glaciol.,* **38,** 261–265.

——, R. Granger, and J. Pomeroy, 2006: Boundary layer growth and advection of heat over snow and soil patches: Modelling and parametrization. *Hydrol. Processes,* **20,** 953–967.

Etchevers, P., 2000: Modélisation de la phase continentale du cycle de l'eau à l'échelle régionale: Impact de la modélisation de la neige sur l'hydrologie du Rhône. Ph.D. thesis, Université Paul Sabatier Toulouse III, 361 pp.

——, and Coauthors, 2003: Validation of the surface energy budget simulated by several snow models (SNOWMIP project). *Ann. Glaciol.,* **38,** 150–158.

Favier, V., P. Wagnon, and P. Ribstein, 2004: Glaciers of the inner and outer Tropics: A different behavior but a common response to climatic forcing. *Geophys. Res. Lett.,* **31,** L16403, doi:10.1029/2004GL020654.

Francou, B., M. Vuille, P. Wagnon, J. Mendoza, and J. E. Sicart, 2003: Tropical climate change recorded by a glacier in the central Andes during the last decades of the 20th century: Chacaltaya, Bolivia, 16°S. *J. Geophys. Res.,* **108,** 1179, doi:10.1029/2002GL014870.

Garreaud, R. D., 2000: Intraseasonal variability of moisture and rainfall over South American Altiplano. *Mon. Wea. Rev.,* **128,** 3337–3346.

Gerbaux, M., C. Genthon, P. Etchevers, C. Vincent, and J. P. Dedieu, 2005: Surface mass balance of glaciers in the French Alps: Distributed modeling and sensitivity to climate change. *J. Glaciol.,* **51,** 561–572.

Granger, R. J., R. Essery, and J. W. Pomeroy, 2006: Boundary layer growth over snow and soil patches: Field observations. *Hydrol. Processes,* **20,** 943–951.

Habets, F., A. Boone, and J. Noilhan, 2003: Simulation of a Scandinavian Basin using the diffusion transfer version of ISBA. *Gobal Planet. Change,* **38,** 137–149.

Kaser, G., 2001: Glacier–climate interaction at low latitudes. *J. Glaciol.,* **47,** 195–204.

——, and H. Osmaston, 2002: *Tropical Glaciers.* International Hydrology Series, UNESCO and Cambridge University Press, 207 pp.

Lejeune, Y., Y. L'Hôte, and P. Chevallier, 2003: Instrumentation et constitution d'une base de données météorologiques et nivologiques dans les Andes; Station Charquini, 4795 m, Bolivie. Météo-France/CNRM, Note de Centre 21, 63 pp. [Available online at http://www.mpl.ird.fr/hydrologie/pch/documents/PNRH01-37/pdf/PNRH0137_note_charquini.pdf.]

——, ——, P. Etchevers, P. Wagnon, J. P. Chazarin, and P. Chevallier, 2006: *Constitution d'une Base de Données Météorologiques sur un Site Andin de Haute Altitude: Le Site du Charquini, 4795 m, Bolivie.* IAHS Red Book Series, IAHS Press, in press.

L'Hôte, Y., P. Chevallier, A. Coudrain, Y. Lejeune, and P. Etchevers, 2005: Relationship between precipitation and air temperature: Comparison between the Bolivian Andes and the Swiss Alps. *Hydrol. Sci. J.,* **50,** 989–997.

Liston, G. E., and M. Sturm, 1998: A snow-transport model for complex terrain. *J. Glaciol.,* **44,** 498–516.

Mölg, T., and D. R. Hardy, 2004: Ablation and associated energy balance of a horizontal glacier surface on Kilimanjaro. *J. Geophys. Res.,* **109,** D16104, doi:10.1029/2003JD004338.

Noilhan, J., and S. Planton, 1989: A simple parametrization of land surface processes for meteorological models. *Mon. Wea. Rev.,* **117,** 536–549.

——, and J.-F. Mahfouf, 1996: The ISBA land surface parameterization scheme. *Global Planet. Change,* **13,** 145–159.

Peters-Lidard, C. D., E. Blackburn, X. Liang, and E. F. Wood, 1998: The effect of soil thermal conductivity parametrization on surface energy fluxes and temperatures. *J. Atmos. Sci.,* **55,** 1209–1224.

Pomeroy, J. W., D. M. Gray, F. R. Shook, B. Toth, R. L. H. Essery, A. Pietroniro, and N. Hedstrom, 1998: An evaluation of snow accumulation and ablation processes for land surface modeling. *Hydrol. Processes,* **12,** 2339–2367.

Roesch, A., M. Wild, H. Gilgen, and A. Ohmura, 2001: A new snow cover fraction parametrization for the ECHAM4 GCM. *Climate Dyn.,* **17,** 933–946.

Rousseau, D., 1980: A new skill score for the evaluation of yes/no forecasts. *Proc. WMO Symp. on Probalistic and Statistical Methods in Weather Forecasting,* Nice, France, World Meteorological Organization, 167–174.

Sicart, J. E., P. Wagnon, and P. Ribstein, 2005: Atmospheric controls of the heat balance of Zongo Glacier (16°S, Bolivia). *J. Geophys. Res.,* **110,** D12106, doi:10.1029/2004JD005732.

Takahara, H., and K. Higuchi, 1985: Thermal modification of air moving over melting snow surfaces. *Ann. Glaciol.,* **6,** 235–237.

Thompson, L. G., E. Mosley-Thompson, M. E. Davis, P.-N. Lin, K. Henderson, and T. A. Mashiotta, 2003: Tropical glacier and ice core evidence of climate change on annual to millennial time scales. *Climatic Change,* **59,** 137–155.

Vuille, M., R. S. Bradley, and F. Keimig, 2000: Interannual climate variability in the central Andes and its relation to tropical Pacific and Atlantic forcing. *J. Geophys. Res.,* **105** (D10), 12 447–12 460.

Wagnon, P., P. Ribstein, B. Francou, and J. E. Sicart, 2001: Anomalous heat and mass budget of Zongo Glacier, Bolivia during the 1997–98 El Niño year. *J. Glaciol.,* **47,** 21–28.